

EVALUATION OF THE α -CASE WITH TiO_2 IN MOLD FOR TITANIUM INVESTMENT CASTING

Seul Lee and Young-Jig Kim 

School of Advanced Materials Science and Engineering, Sungkyunkwan University, Suwon, Gyeonggi-do, Republic of Korea

Copyright © 2016 American Foundry Society
DOI 10.1007/s40962-016-0093-8

Abstract

Molten titanium easily reacts with not only oxygen, carbon, and nitrogen but also the ceramic mold to form an α -case on the casting surface. However, the brittle α -case must be removed by chemical milling because it weakens the mechanical properties of the casting. The aim of this study is to evaluate and suppress the formation of the α -case by including TiO_2 in the mold. Titanium powder was added into the alumina mold in order to facilitate the formation of TiO_2 by the oxidation of titanium during mold firing. Another way to include TiO_2 in the mold was to simply add TiO_2 into the alumina mold. Optical microscopy and the micro-Vickers hardness test were used to characterize the

α -case. The composition and morphology of the molds were confirmed using X-ray diffraction and field emission scanning electron microscopy. The mold with added titanium ($\text{Al}_2\text{O}_3 + \text{Ti}$) was effective in controlling the α -case. However, the interfacial reactions of the mold with the added TiO_2 ($\text{Al}_2\text{O}_3 + \text{TiO}_2$) exhibited distinct differences in α -case formation compared to the Ti-added mold ($\text{Al}_2\text{O}_3 + \text{Ti}$), while having almost identical compositions.

Keywords: titanium, investment casting, ceramic mold, α -case

Introduction

The investment casting process shows outstanding reproducibility of castings within close dimensional limits.¹ Because of the poor machinability and workability of titanium, investment castings are widely used to produce complex and near-net-shaped products. However, titanium is extremely reactive with ceramic molds, resulting in the formation of the α -case. The α -case is formed by the diffusion of oxygen and metallic elements in the ceramic mold and is composed of titanium oxide and intermetallic compounds.² The formation of the α -case on castings degraded the fatigue and ductility by acting as surface crack initiation sites under the service temperature.³ Therefore, the α -case is usually removed through chemical milling before use. However, the milling process is expensive and limits the dimensional tolerance. Al_2O_3 was selected for the mold material because Al_2O_3 is more cost effective than ZrO_2 and Y_2O_3 . In addition, Al_2O_3 features suitable strength, permeability, and collapsibility, which can ensure dimensional accuracy of castings.⁴ The aim of this study is to evaluate and control

the formation of α -case by the inclusion of TiO_2 in the Al_2O_3 mold, which is a primary component of the α -case in the mold. The inclusion of TiO_2 in the mold was achieved by the oxidation of titanium during the mold firing processes or it was added during the mold manufacturing process.

Experimental Procedures

Alumina (Al_2O_3 , purity of 99 %, 325 mesh), titanium (Ti, purity of 99 %, 325 mesh), rutile titanium dioxide (TiO_2 , purity of 99 %, 325 mesh), and colloidal SiO_2 (30 % SiO_2 , 15 nm) were used as primary coating materials. In order to produce TiO_2 in the mold, 50 wt% of titanium or TiO_2 was added to the Al_2O_3 flour (denoted as $\text{Al}_2\text{O}_3 + 50\text{Ti}$ and $\text{Al}_2\text{O}_3 + 50\text{TiO}_2$ respectively.) Subsequently, colloidal SiO_2 was added to the slurry until it achieved a viscosity in 40 s, as measured using a Zahn cup (ASTM D-4212). The primary coating process was repeated twice, and the manufacturing condition of the slurry is shown in Table 1. In addition, the chamotte ($\text{Al}_2\text{O}_3 \cdot \text{SiO}_2$, purity of 98 %, 325 mesh) and colloidal

Table 1. Manufacturing Condition of Primary Coat

| Mold | Primary coat | | | | |
|---|---|-------------|--------------------------------|-------------|-----------------------------|
| | Flour | Size (mesh) | Stucco | Size (mesh) | Mixing ratio (flour/binder) |
| Al ₂ O ₃ | Al ₂ O ₃ | 325 | Al ₂ O ₃ | 200 | 100:32 |
| Al ₂ O ₃ + 50TiO ₂ | Al ₂ O ₃ , TiO ₂ | 325 | | | 100:32 |
| Al ₂ O ₃ + 50Ti | Al ₂ O ₃ , Ti | 325 | | | 100:34 |

SiO₂ were used as backup slurry materials. A backup coating was applied three times, at 4 h intervals, with chamotte slurry and Al₂O₃ stucco (purity of 99 %, 18–32 mesh). The mold was dewaxed in an autoclave at 150 MPa and fired in the furnace at 1200 K (927 °C/ 1700 °F) for 2 h in an air atmosphere. One hundred and twenty grams of commercial pure titanium (ASTM B-348, grade 2) was placed on top of a water-cooled copper crucible. The mold was located inside the copper crucible for dropping titanium melts. A titanium rod was melted in a plasma arc melting furnace (PAM), and the casting process is presented in Figure 1. Phase identification of molds was carried out by X-ray diffraction (XRD, M18XHF-SRA, Mac Science). The thickness of the α-case was determined by using a micro-Vickers hardness test (MVK-H2, Mitutoyo) and optical microscopy (OM, PME 3, Olympus). In our work, the micro-Vickers hardness test was performed at an interval of 50 μm from the casting surface to 1000 μm, applying a 100 g load. The microstructure and composition of the mold surface before and after casting were examined by field emission scanning electron microscopy (FE-SEM, JSM-7600F, JEOL). Also, the surface roughness of the before casting molds was confirmed using a profiler (Bruker DXT-A, Bruker).

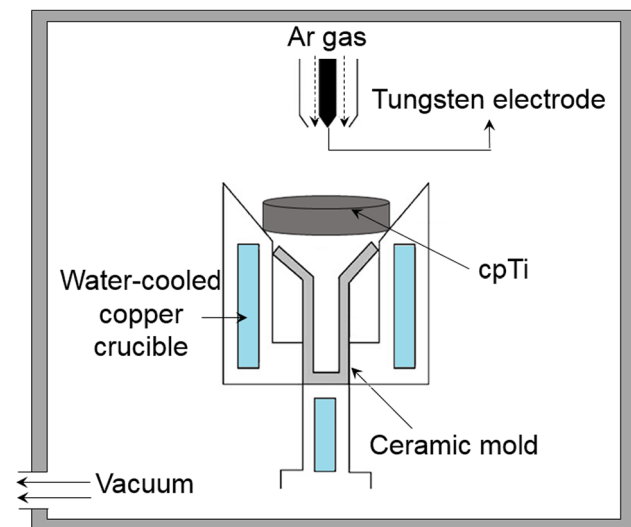
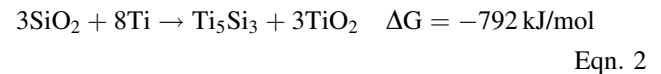
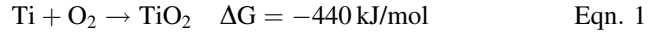


Figure 1. Plasma arc melting furnace used to produce the titanium castings.

Results and Discussion

Analysis of Mold Composition

Figure 2 shows the X-ray diffraction (XRD) spectra of the ceramic molds. The composition of the Al₂O₃ and Al₂O₃ + 50TiO₂ molds was unchanged, indicating that the Al₂O₃ and TiO₂ were in stable phases after mold firing. However, the large amount of Al₂O₃, TiO₂, and the small amount of Ti₅Si₃ were found in the Al₂O₃ + 50Ti mold. Most of the TiO₂ was formed by the reaction between atmospheric oxygen and titanium during mold firing. Also, the reaction between titanium and colloidal silica resulted in the formation of Ti₅Si₃ and TiO₂. The Gibbs free energy changes (ΔG) of TiO₂ and Ti₅Si₃ at 1200 K (927 °C/ 1700 °F) in the Al₂O₃ + 50Ti mold are shown in the following equation:⁵



Thermodynamic calculations indicated that the formation of TiO₂ and Ti₅Si₃ were spontaneous reactions. From the XRD results, the main composition of the Al₂O₃ + 50Ti

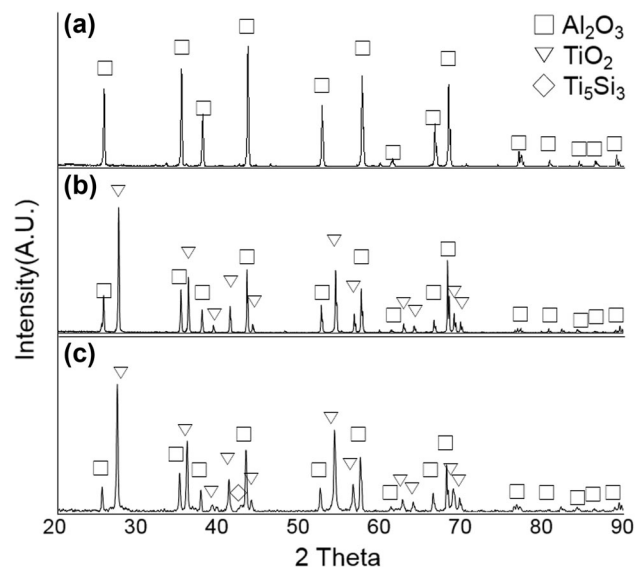


Figure 2. XRD results of the ceramic mold (a) Al₂O₃, (b) Al₂O₃ + 50TiO₂, and (c) Al₂O₃ + 50Ti.

mold was found to be very similar to that of the $\text{Al}_2\text{O}_3 + 50\text{TiO}_2$ mold, with Al_2O_3 and TiO_2 being present in both molds.

Thickness of α -Case

Figure 3a and 3b shows a severe reaction layer that had Widmanstätten microstructures made from Al_2O_3 and $\text{Al}_2\text{O}_3 + 50\text{TiO}_2$ molds. However, the titanium surface made with the $\text{Al}_2\text{O}_3 + 50\text{Ti}$ mold (see Figure 3c) had the same microstructure as the inner side of the casting. This indicates that the use of the $\text{Al}_2\text{O}_3 + 50\text{Ti}$ mold effectively suppressed the formation of the α -case. Figure 4 exhibits a micro-Vickers hardness profile in titanium castings in relation to the depth from the surface. The depth of the α -case was revealed to be 350 μm when the castings were made using Al_2O_3 and $\text{Al}_2\text{O}_3 + 50\text{TiO}_2$ molds. However, for titanium castings made with the $\text{Al}_2\text{O}_3 + 50\text{Ti}$ mold, the thickness of the α -case was only 50 μm . The formation of the α -case was entirely different in the $\text{Al}_2\text{O}_3 + 50\text{TiO}_2$ and $\text{Al}_2\text{O}_3 + 50\text{Ti}$ molds although the compositions of the molds were almost similar.

The Morphology of Mold Surface Before the Casting

The mold surface morphology and chemical compositions were analyzed by FE-SEM in order to understand the reason why $\text{Al}_2\text{O}_3 + 50\text{Ti}$ leads to less α -case formation. Figures 5 and 6 show FE-SEM images and energy dispersive spectroscopy (EDS) results of the mold surface before casting. Before casting, the Al_2O_3 mold surface contained homogeneously distributed, Al_2O_3 and SiO_2 . Because the fine flour particles surrounded by colloidal silica formed a chemical bonding between the large flours. Contact between the larger ceramic particles is achieved through small bridges of binder and flour.⁶

The $\text{Al}_2\text{O}_3 + 50\text{TiO}_2$ mold surface also consisted of a mixture of Al_2O_3 and SiO_2 ($\text{Al}_2\text{O}_3 + \text{SiO}_2$) or TiO_2 and SiO_2 ($\text{TiO}_2 + \text{SiO}_2$) that could not be distinguished by

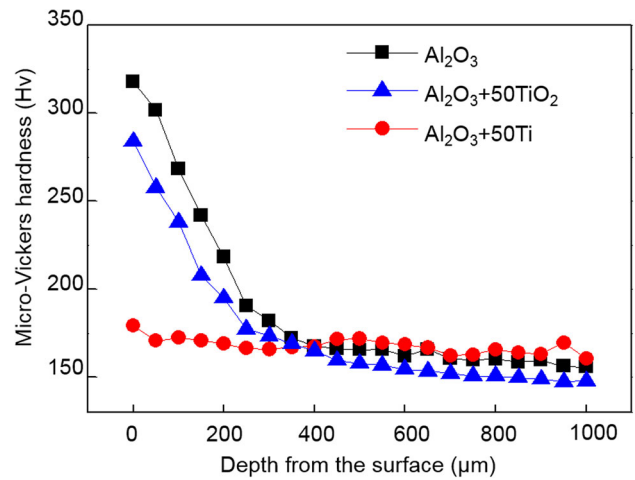


Figure 4. Micro-Vickers hardness profile, as a function of depth from the surface, for titanium casting in ceramic molds.

their morphologies. In addition, $\text{Al}_2\text{O}_3 + \text{SiO}_2$ and $\text{TiO}_2 + \text{SiO}_2$ both had flat surfaces.

In the $\text{Al}_2\text{O}_3 + 50\text{Ti}$ mold, the TiO_2 phase had a flaky and rough surface, in conjunction with a flat surface of $\text{Al}_2\text{O}_3 + \text{SiO}_2$ layer. With an increase in temperature during mold firing, all surfaces of added titanium powder were covered by an oxide layer of flaky form because of titanium oxidation in $\text{Al}_2\text{O}_3 + 50\text{Ti}$ mold.⁷ The roughness of mold surface was characterized by the average displacement from the mean height of asperities R_a for comparison between the added TiO_2 and formed TiO_2 (R_a = arithmetic average roughness). The average surface roughness of Al_2O_3 mold was 0.96 μm . And the R_a of $\text{Al}_2\text{O}_3 + \text{TiO}_2$ mold was 0.97 μm , which is approximately equal value to Al_2O_3 mold. However, the roughness of $\text{Al}_2\text{O}_3 + 50\text{Ti}$ mold was 1.18 μm and this value is slightly higher than Al_2O_3 and $\text{Al}_2\text{O}_3 + 50\text{TiO}_2$ molds. The titanium oxidation during mold firing results in the increase of surface roughness in $\text{Al}_2\text{O}_3 + 50\text{Ti}$ mold. However, increased roughness would not have a great effect on the dimensional tolerance because the augmented roughness was a low value.

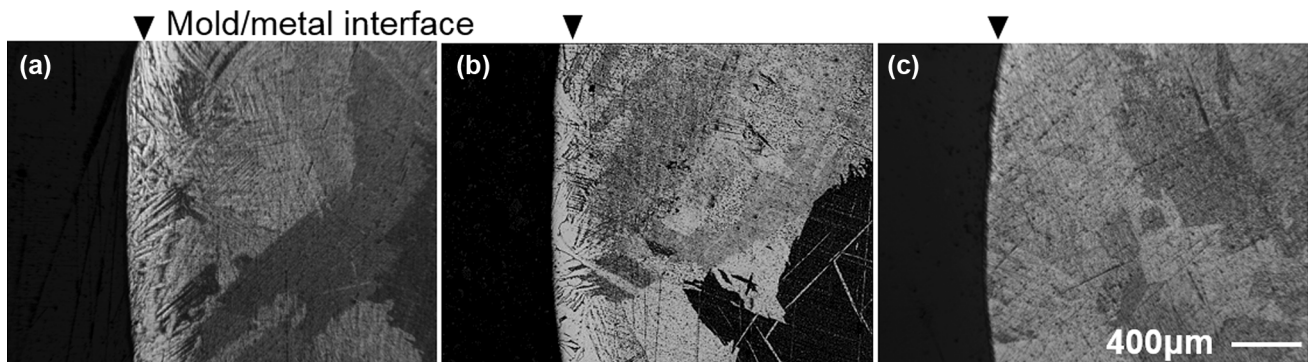


Figure 3. Microstructure from titanium castings made in the ceramic molds (a) Al_2O_3 , (b) $\text{Al}_2\text{O}_3 + 50\text{TiO}_2$, (c) $\text{Al}_2\text{O}_3 + 50\text{Ti}$.

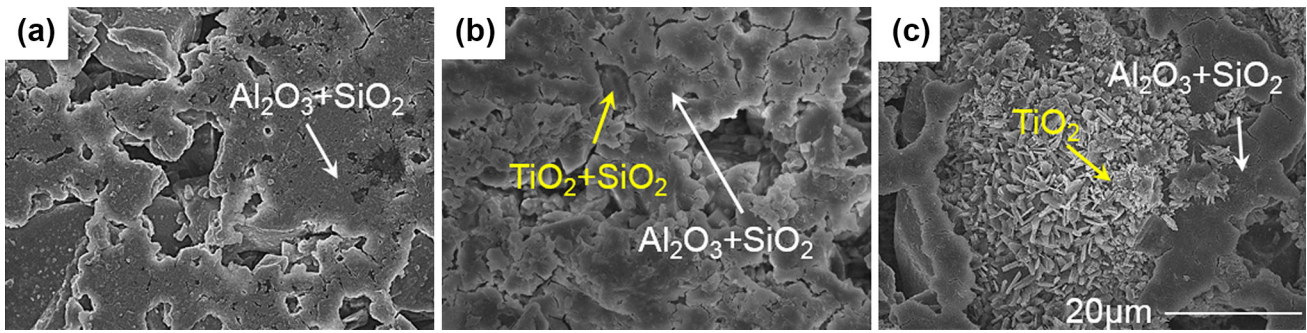


Figure 5. FE-SEM images of the mold surface of before casting (a) Al_2O_3 , (b) $Al_2O_3 + 50TiO_2$, (c) $Al_2O_3 + 50Ti$.

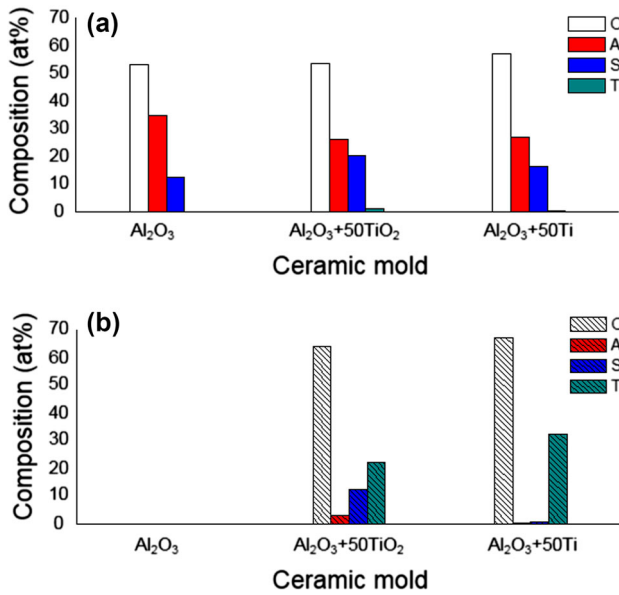


Figure 6. EDS results of the ceramic mold surface before casting (a) the region of $Al_2O_3 + SiO_2$, (b) the region of TiO_2 or $TiO_2 + SiO_2$.

The Morphology of Mold Surface After the Casting

The morphology and composition analysis of molds after casting are presented in Figures 7 and 8. After casting in the Al_2O_3 mold, the primary coating layer of $Al_2O_3 + SiO_2$ was no longer observed because the titanium melt reacts with the Al_2O_3 mold by dissolving the

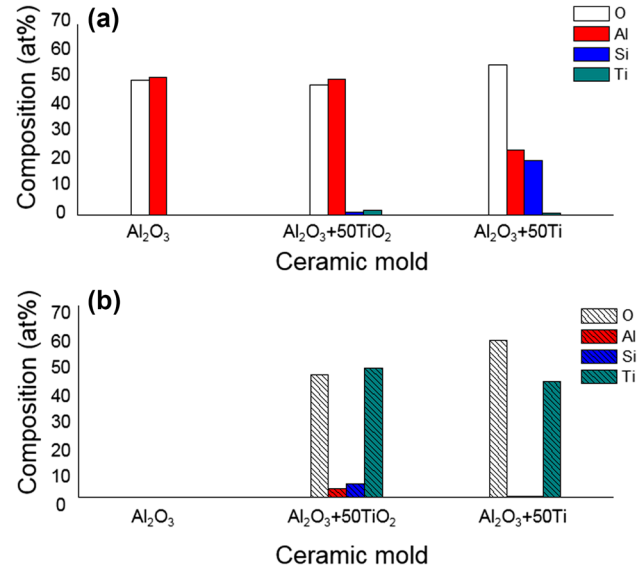


Figure 8. EDS results of the ceramic mold surface after casting (a) the region of $Al_2O_3 + SiO_2$, (b) the region of TiO_2 or $TiO_2 + SiO_2$.

$Al_2O_3 + SiO_2$ layer by penetration. The $Al_2O_3 + SiO_2$ layer was detached during the knockout, resulting in titanium that adheres to the $Al_2O_3 + SiO_2$. And the coarse Al_2O_3 flour in the Al_2O_3 mold had a ratio of aluminum to oxygen of one-to-one ratio.

Similarly, the primary coating layers of $Al_2O_3 + SiO_2$ and $TiO_2 + SiO_2$ were not observed, along the same lines as the Al_2O_3 mold. The exposed TiO_2 and Al_2O_3 were coarse

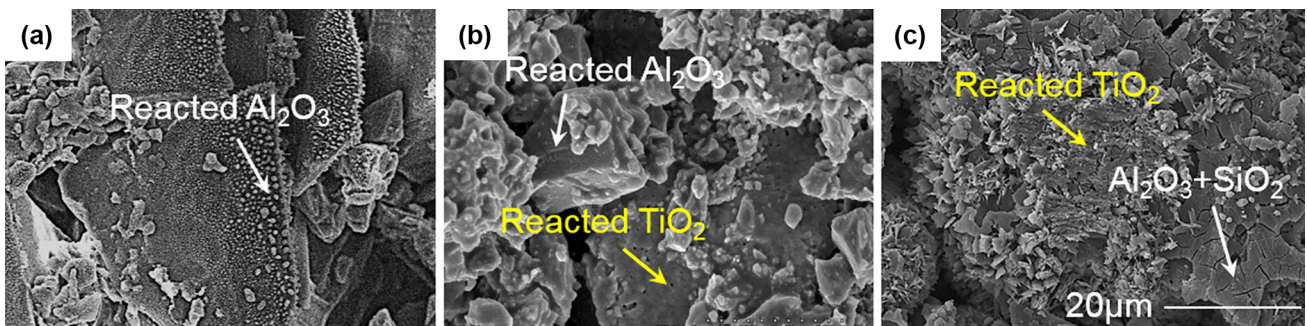


Figure 7. FE-SEM images of the mold surface of after casting (a) Al_2O_3 , (b) $Al_2O_3 + 50TiO_2$, (c) $Al_2O_3 + 50Ti$.

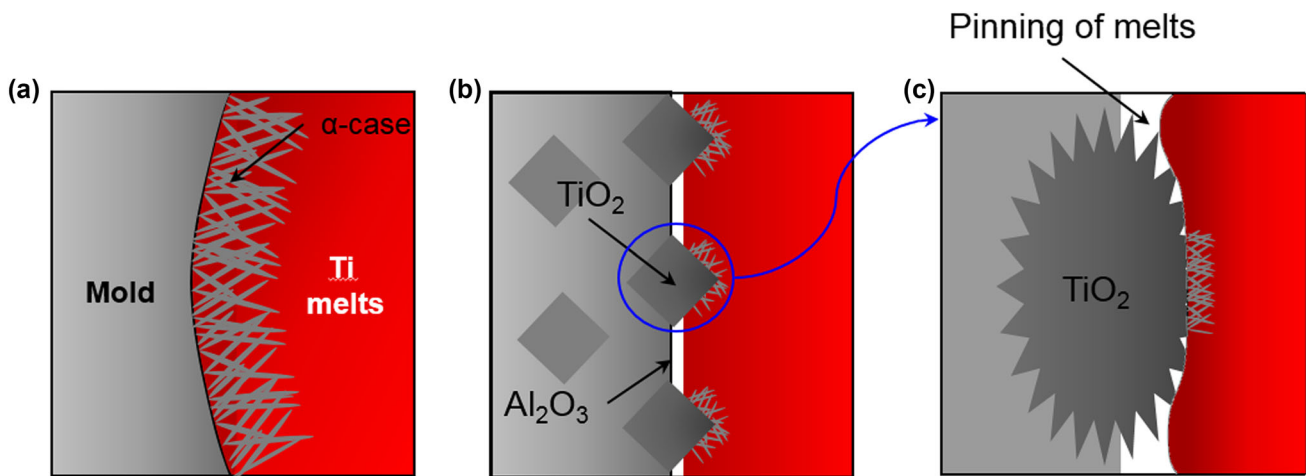


Figure 9. Diagram illustrating the reactions of titanium with (a) Al_2O_3 and $\text{Al}_2\text{O}_3 + 50\text{TiO}_2$, (b) $\text{Al}_2\text{O}_3 + 50\text{Ti}$, (c) macrophotography of TiO_2 region in $\text{Al}_2\text{O}_3 + 50\text{Ti}$.

refractory flours that existed inside the primary coating layers, and the ratio of metal to oxygen was almost 1:1.

In addition, the morphology of the TiO_2 phase was changed in the $\text{Al}_2\text{O}_3 + 50\text{Ti}$ mold. Since the TiO_2 in $\text{Al}_2\text{O}_3 + 50\text{Ti}$ was in contact with the titanium melt, the shape of TiO_2 surface flattens. However, inner coarse flour was not exposed, unlike the Al_2O_3 or $\text{Al}_2\text{O}_3 + 50\text{TiO}_2$ mold. The ratio of titanium to oxygen was decreased, due to the rapid diffusion of oxygen into the titanium melts in the $\text{Al}_2\text{O}_3 + 50\text{Ti}$ mold. As a result, a change in the ratio of mold composition occurred during casting. However, the shape and chemical composition of the primary coating layer of $\text{Al}_2\text{O}_3 + \text{SiO}_2$ remained intact in the $\text{Al}_2\text{O}_3 + 50\text{Ti}$ mold. And this result considered that the $\text{Al}_2\text{O}_3 + \text{SiO}_2$ had no contact with the titanium melt.

Effect of Formed TiO_2 in $\text{Al}_2\text{O}_3 + 50\text{Ti}$ mold on α -Case Formation

The surface morphology change (depending on the before and after casting), formed TiO_2 in the $\text{Al}_2\text{O}_3 + 50\text{Ti}$ mold, that had a rougher surface than the $\text{Al}_2\text{O}_3 + \text{SiO}_2$ layer, due to the titanium oxidation. The rough surface results in an increase of wetting angle or resistance between the melts and substrate due to the reduction of contact area. Thus, the reaction rate may decline with rough surface.⁸ Also, Sobczak et al.⁹ have reported that rough surface may pin the triple line and strongly influence the wetting angle without notably influencing R_a , which may lead to $\Delta\theta$ values as high as 30° . (Triple line is the line of contact between the solid, liquid & atmosphere). As a result, the surface roughness could affect the wetting angles by decreasing reaction rate. Furthermore, the refractory materials that have good resistance to wetting by melts are worthwhile because the reaction can only occur if both make contact. A refractory which has good resistance to

wetting has a tendency to increase its resistance to reaction.¹⁰ Therefore, the formed TiO_2 by increasing surface roughness suppressed the contact of titanium melts with $\text{Al}_2\text{O}_3 + 50\text{Ti}$ mold. A schematic showing the reactions that lead to the formation of the α -case is illustrated in Figure 9. When the titanium melts were poured into the Al_2O_3 and $\text{Al}_2\text{O}_3 + 50\text{TiO}_2$ molds, the titanium melts were exposed to the entire area of the mold surface. The molds decomposed into Al, O, Si, or Ti, and then these elements diffused into the titanium melt to form the α -case.^{11–13} However, titanium was mainly in contact with formed TiO_2 because the morphology of TiO_2 was rougher and protruded more than the $\text{Al}_2\text{O}_3 + \text{SiO}_2$ layer.

Conclusions

The composition of $\text{Al}_2\text{O}_3 + 50\text{Ti}$ and $\text{Al}_2\text{O}_3 + 50\text{TiO}_2$ molds was found to be nearly identical due to titanium oxidation during mold firing. However, the morphology of the $\text{Al}_2\text{O}_3 + 50\text{TiO}_2$ mold resembled that of the Al_2O_3 mold. Further, the reactivity of titanium with $\text{Al}_2\text{O}_3 + 50\text{TiO}_2$ was similar to that with the Al_2O_3 mold. However, a reaction between the $\text{Al}_2\text{O}_3 + 50\text{Ti}$ mold and titanium rarely occurred. These results indicate that the formed TiO_2 inhibits contact with the melt due to the increase in surface roughness.

REFERENCES

1. P.R. Beeley, R.F. Smart, *Investment Casting*, 1st edn. (Institute of Materials, London, 1995), pp. 23–24
2. S.Y. Sung, B.J. Choi, B.S. Han, H.J. Oh, Y.J. Kim, *J. Mater. Sci. Technol.* **24**, 70 (2008)
3. K.F. Lin, C.C. Lin, *J. Mater. Sci.* **34**, 5899 (1999)

4. M.G. Kim, S.Y. Sung, Y.J. Kim, *Mater. Trans.* **45**, 536 (2004)
5. I. Barin, G. Platzki, *Thermochemical Data of Pure Substances*, 3rd edn. (VCH Publishers, New York, 1995)
6. S. Jones, P.M. Marquis, *Br. Ceram. Trans.* **94**, 68 (1995)
7. V.V. Tavgen, E.V. Shinkareva, E.V. Karpinchik, YuG Zonov, *Sov. Powder Metall. Metal Ceram.* **31**, 193 (1992)
8. J. Zhu, A. Kamiya, T. Yamada, W. Shi, K. Naganuma, K. Mukai, *Mater. Sci. Eng., A* **327**, 117 (2002)
9. N. Sobczak, M. Singh, R. Asthana, *Curr. Opin. Solid State Mater. Sci.* **9**, 241 (2005)
10. J.P. Kuang, R.A. Harding, J. Campbell, *J. Mater. Sci. Technol.* **16**, 1007 (2000)
11. C. Frueh, D.R. Poirier, M.C. Maguire, *Metall. Mater. Trans. B* **28**, 919 (1997)
12. K.S. Chan, M. Koike, B.W. Johnson, T. Okabe, *Metall. Mater. Trans. A* **39**, 171 (2008)
13. W.J. Boettinger, M.E. Williams, S.R. Coriell, U.R. Kattner, B.A. Mueller, *Metall. Mater. Trans. B* **31**, 1419 (2000)